

Article

A Lower Limb Rehabilitation Robot with Rigid-Flexible Characteristics and Multi-Mode Exercises

Mingjie Dong , Jianping Yuan and Jianfeng Li * 

Beijing Key Laboratory of Advanced Manufacturing Technology, Faculty of Materials and Manufacturing, Beijing University of Technology, Beijing 100124, China

* Correspondence: lijianfeng@bjut.edu.cn

Abstract: Lower limb rehabilitation robot (LLRR) can effectively help restore the lower limb's motor function of patients with hemiplegia caused by stroke through a large number of targeted and repetitive rehabilitation training. To improve the safety and comfort of robot-assisted lower limb rehabilitation, we developed an LLRR with rigid-flexible characteristics; the design of passive joints is used to improve human-machine compatibility; the design of flexible unit makes the mechanism have certain rigid-flexible characteristics. Three different rehabilitation training methods have been developed to adapt to the patients at different stages of rehabilitation, namely, passive exercise, active exercise and resistance exercise, respectively. Experiments with healthy subjects have been conducted to verify the effectiveness of the development of the different training modes of the LLRR, showing good compatibility of the mechanism and good trajectory tracking performance of the developed training methods.

Keywords: lower limb rehabilitation robot; rigid-flexible; passive joint; rehabilitation training



Citation: Dong, M.; Yuan, J.; Li, J. A Lower Limb Rehabilitation Robot with Rigid-Flexible Characteristics and Multi-Mode Exercises. *Machines* **2022**, *10*, 918. <https://doi.org/10.3390/machines10100918>

Academic Editor: Dan Zhang

Received: 19 September 2022

Accepted: 7 October 2022

Published: 10 October 2022

Publisher's Note: MDPI stays neutral with regard to jurisdictional claims in published maps and institutional affiliations.



Copyright: © 2022 by the authors. Licensee MDPI, Basel, Switzerland. This article is an open access article distributed under the terms and conditions of the Creative Commons Attribution (CC BY) license (<https://creativecommons.org/licenses/by/4.0/>).

1. Introduction

Stroke has a poor prognosis and is becoming the leading cause of permanent disabilities worldwide, with over 15 million new cases each year and 50 million stroke survivors, which can cause neurological and functional impairments and affect the patients' daily activities [1]. Most stroke survivors have lower limb mobility deficits [2]. For the reason that manually assisted training for lower limbs requires intensive labor from the physical therapist, many different lower limb rehabilitation robots (LLRRs) have been developed in the last two decades, such as those commercial products including LOPES [3], ALEX [4], ReWalk [5], Indego [6], et al. In addition, many other LLRRs have also been studied with different mechanisms for different application scenarios and patient populations.

To design and analyze the configuration of the mechanical structure from different perspectives and face different application scenarios, many researchers have developed LLRRs. A passive lower limb exoskeleton with hip and knee joint is proposed for walking assistance to save powers and reduce the LLRR's weight and its complexity of the mechanism, which is designed with built-in spring mechanisms for gravity compensation of the human leg [7]. To help patients quickly and accurately transmit the motion intention to the robot and reduce the possibility of falls and errors, Liu et al. developed a vision-assisted autonomous lower-limb exoskeleton robot based on the principles of human visual feedback and motion decision-making [8]. To reduce the size and mass of the conventional LLRRs, Wang et al. developed a hybrid end-traction LLRR by using the hybrid mechanism $(2 - UPS + U) \& (R + RPS) \& (2 - RR)$ and a mirror motion actuator [9]. To deliver post-stroke therapy to both upper and lower extremities, Chole et al. developed an active mobile end-effector foot-plate/handle grip robot, which has features including dual-usability, lightweight design, mechanically adjustable maximum forces and torques, inherent safety, portability, and teleoperation capability [10]. To probe and promote motor adaptation and volitional movement, Alexander et al. developed one degree of freedom

(DOF) rehabilitation robot named NOTTABIKE, which can render both impedance- and admittance-based haptic environments with accuracy and responsiveness that are useful for the study of human coordination and the delivery of rehabilitative therapy [11]. In addition to the different configurations, different control strategies have been developed for LLRRs, to improve their gait training performance using passive exercise or improve the rehabilitation training performance with patient-active exercise. From the above researches, we can see that although many different mechanisms related to LLRR have been studied, relatively little has been done with rigid-flexible characteristics.

In addition to the mechanism design, the control algorithms of the LLRRs are also very important. To overcome the situation that the patients must acquire the ability to maintain their balance and shift their weight using forearm crutches, which is challenging for paraplegics, Ma et al. proposed an automated intelligent gait planning method that integrated a finite-state machine model as an underlying foundation and a gait generation model in addition to the exoskeleton system [12]. To target a specific muscle group during a functional task such as simulated walking, the indirect control scheme based on a computational model of the human musculoskeletal system is proposed in [13], which searches for the optimal load along the predefined path to maximize the efficiency of muscle training. To achieve the predetermined angular trajectories, the Lyapunov adaptive and swarm-fuzzy logic control strategy was implemented on a 4-DOF lower limb assistive robot, in which the control law is an integration of swarm-fuzzy logic control (SFLC) and Lyapunov adaptive control (LAC) that are improved by particle swarm optimization (PSO) [14]. To improve the safety and tracking performance of an LLRR, Liu et al. presented an application of the variable stiffness actuator (VSA)-based assistance/rehabilitation robot-featured impedance control using a cascaded position torque control loop; The robot follows the adaptive impedance control paradigm, thereby achieving an adaptive assistance level according to human joint torque [15]. To plan the subject's desired trajectory based on interaction force during physical human-robot interaction, Zhou et al. developed a trajectory deformation algorithm as a high-level trajectory planner, which can improve robot compliance and movement smoothness [16]. To solve the problem that a significant gait deviation may occur between the gait trajectory of the wearer and the reference trajectory, Zhang et al. proposed a gait deviation correction method to decrease the gait deviation for lower limb exoskeleton robots [17]. Although many control strategies of the LLRRs as mentioned above have been studied, we can see that most of the research is aimed at improving the performance of gait planning and trajectory tracking, and few studies on multimodal rehabilitation training methods have been carried out.

In this work, we developed an LLRR with rigid-flexible characteristics and multi-mode exercises based on our previous researches on rehabilitation robot, including improving the compatibility of upper limb rehabilitation robot with improved mechanism [18] and developing different rehabilitation training methods with compliance control [19]. The paper is organized as follows. Section 2 demonstrates the mechanism design with rigid-flexible characteristics. Section 3 presents the control system and multi-mode rehabilitation training methods in detail. Experiments and results are displayed and discussed in Section 4, while conclusion is drawn in Section 5.

2. Mechanism Design with Rigid-Flexible Characteristics

2.1. Mechanism Design and Compatibility

The prototype of the LLRR mainly consists of the hip support assembly, left and right leg motion systems, and leg bindings. Both sides of the hip support assembly are connected with the left and right leg motion systems, respectively. The components of the left and right leg motion systems are completely symmetrical and identical. Each motion system has a hip joint drive unit, a knee joint drive unit, and a lower limb link (thigh, calf, and foot). The hip joint drive unit and the knee joint drive unit are respectively driven to rotate by motors, and the leg links connect and support the drive units. In addition, the leg bindings are used to connect the human's lower limbs and the LLRR. The detailed mechanical design

of the LLRR is shown in Figure 1, wherein, the hip support assembly has a fixed support seat, a pair of prismatic pairs, and a pair of sliding pairs, and the distal ends of the two sides are connected with the hip joint drive unit. Due to the symmetry of the LLRR's structure, one side is taken as an example for description. The hip joint driving unit is connected with a thigh link, one side of the knee joint drive unit is connected with the thigh link and the other side is connected with the calf link. Both the thigh link and the calf link are provided with a chute, which can form a prismatic pair with the output rods of the hip joint and knee joint drive units, respectively. The length of the leg link can be fixed by bolts when the robot works.

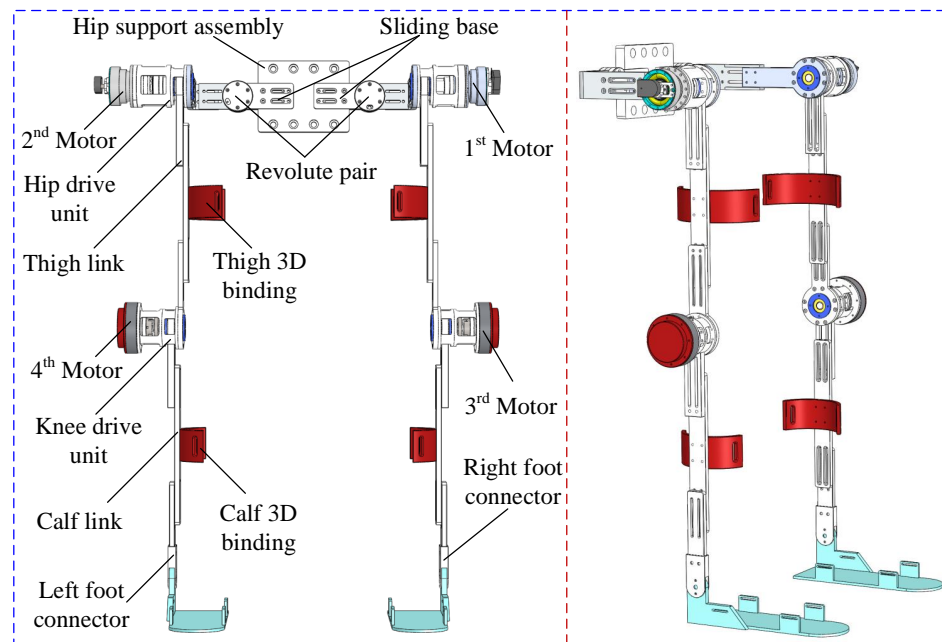


Figure 1. Mechanism design of the lower limb rehabilitation robot.

In order to realize the human-machine compatibility of human hip and knee joints in rehabilitation training, we specially added corresponding passive joints in the mechanism design. The revolute pair in the hip support assembly allows the left and right leg motion systems to carry out adduction and abduction movements; the calf binding and the calf link have a sliding pair, which makes the LLRR's knee joint and the human's knee joint indistinguishable during the movement, with no special adjustment of center axis alignment required. Based on the sliding pair and the revolute pair mentioned above, the LLRR can generate passive deflection of the displacement and angle within a certain range to compensate for the error of the human-machine joint, thereby improving the compatibility between the human and the robot. By adjusting the hip support component and the prismatic pair in the leg link, the length of the LLRR's hip and legs can be adjusted according to the different body sizes of the patients. The adjustment range of the hip width is 39~47 cm, the leg length is 75~100 cm, and the height is 155~180 cm, thereby improving the versatility of the robot.

2.2. Principle and Implementation of the Rigid-Flexible Characteristics

To enhance the safety of the LLRR from the mechanism design, a flexible joint is mounted in the knee drive unit, with one end fixed to the motor output shaft and the other end fixed to the leg link. The purpose of the design is to transmit the torque from the motor to the leg link, and to provide a buffer space between the motor and the joint, thus increasing the compliance of the mechanism.

Usually, rigid joints are used to ensure precise motion trajectories, while in the mechanism, the torsion springs are connected in series in flexible joints to achieve compliance.

The rigid-flexible characteristics of the LLRR are obtained by the combined design of rigid components and torsion springs. As shown in Figure 2, the flexible joint consists of a torsion spring and two rigid wheels (made of aluminum alloy material) in series, which have the same axis of rotation. The driven wheel has a first limit block which is connected with the output shaft, while the driving wheel has a first limit block and a chute, which is connected to the motor. The torsion spring is arranged between the driving wheel and the driven wheel, and the torsion arms of the torsion spring are staggered, and the first limit block and the second limit block are clamped in the two torsion arms. Because of the existence of the spring, the second limit block in the initial position is located in the middle of the chute and does not contact the driving wheel. When the motor drives the driving wheel to rotate, the driving wheel and the driven wheel rotate relative to each other, and the second limit block is not in contact with the chute. At this time, the first limit block on the driving wheel drives one torsion arm of the torsion spring to rotate, the other torsion arm drives the second limit block to rotate, and the driving wheel and the driven wheel transmit torque through the torsion spring. When the second limit block is in contact with the chute, the driving wheel, and the driven wheel are approximately fixed together and can be regarded as a rigid whole. At this time, the driving wheel directly transmits the torque to the driven wheel to drive it to rotate. Since the second limit block can only rotate in the chute of the driving wheel, the range of the torque provided by the torsion spring for the second limit block is within a fixed α angle.

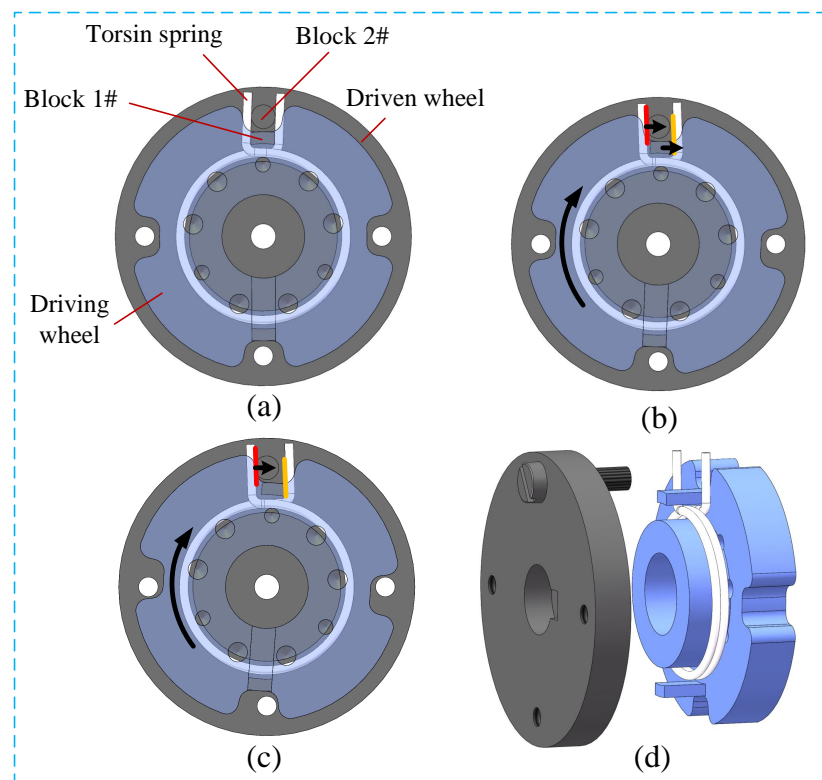


Figure 2. Mechanism design of the flexible unit. (a) the mechanical design; (b) the initial state of the unit; (c) the final state of the unit; (d) 3D explosion view.

In the selection of the torsion spring, a torsion spring with a wire diameter of 1.5 mm, an angle width of 20° , and an outer diameter of 34 mm is used. After being assembled to the driving wheel, it has a torsion range of $\pm 3^\circ$. When the torsion angle of the joint exceeds the set value, the transmission between the driving wheel and the driven wheel changes from flexibility to rigidity. Using this structure as the connection between the motor and the leg drive rod allows the patient's joints to still have room for adjustment during the rehabilitation training process. Therefore, although a small amount of position

control accuracy is sacrificed when the motor drives the leg link to drive the lower limbs of the human body, its property of storing and releasing torque acts as a buffer and shock absorber for joint rotation, thus to reduce the discomfort caused by limbs being bound and improve the compliance and compatibility.

2.3. Design of the Driving Unit

The developed LLRR has four active driving units, including two hip joint driving units and two knee joint driving units. The hip joint units are as shown in Figure 3a, which are driven by two servo motors (TBMS-6013-A00, Kollmorgen, Waltham, MA, USA), with each servo motor providing a torque of 0.413 Nm. The servo motors are also deployed with harmonic reducers (LHD-17-100-C-I, Leader Harmonious Drive Systems Co., Ltd., Suzhou, China, with a reduction ratio of 1:100), thus can output a maximum torque of 41.3 Nm, which can provide a strong power for the LLRR to drive the lower limbs of the human body. On each side, the reducer is fixedly connected to a torque sensor (M2210E, SRI, Nanning, China, with a capacity of 60 Nm) through the flange, and the other side of the torque sensor is fixedly connected to the main shaft R1, so the main shaft and the servo motor at the hip joint are rigidly connected. The knee joint units are as shown in Figure 3b, which are driven by two joint motors with internal drive (HT-03, HAITAI Electromechanical Co., Ltd., China, with continuous torque 6.9 Nm). The motor output shaft is directly connected to the torque sensor (M2210E, SRI, Nanning, China), the other side of the torque sensor is fixedly connected to the driving wheel of the flexible joint, and the driven wheel of the flexible joint is fixedly connected to the main shaft; Therefore, there is a flexible connection between the motor at the knee joint and the main shaft. All the four motors are deployed with incremental encoders to obtain the corresponding angular velocity and angular acceleration.

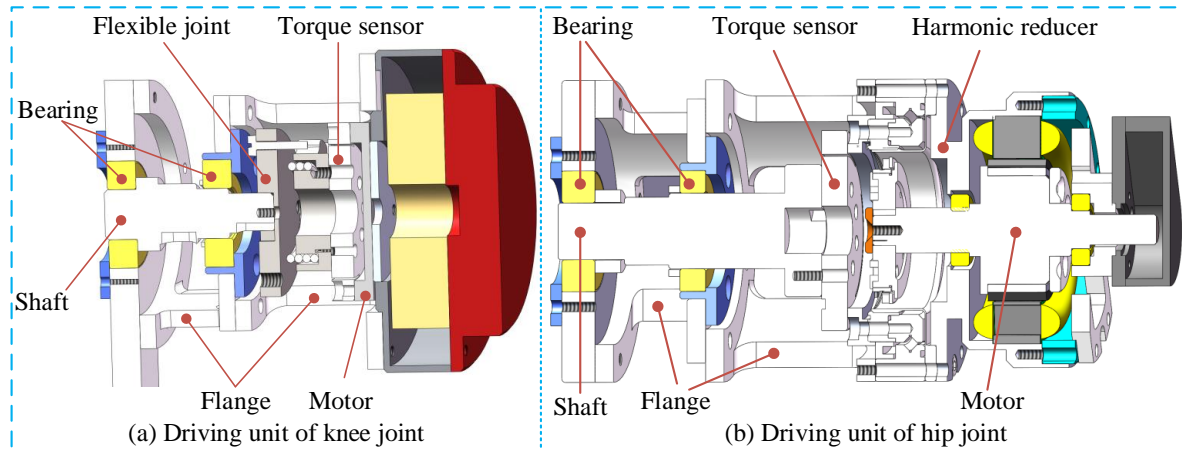


Figure 3. Design of the driving unit.

3. Control System and Multi-Mode Rehabilitation Training Methods

3.1. Control System of the LLRR

The LLRR adopts the master-slave distributed control, which mainly includes human-computer interface, STM32 microprocessor, servo motor drives, servo motors, and torque sensors, with the whole control system shown as in Figure 4. The two servo motors in the hip joint units are driven by two DGFox DX060 drives (HDT, Monte Di Malo, Vicenza, Italy), which have good interpolated position modes using the CANopen DS402 Protocol. The torque sensors and the encoders are used to collect torque and angle information of the LLRR.

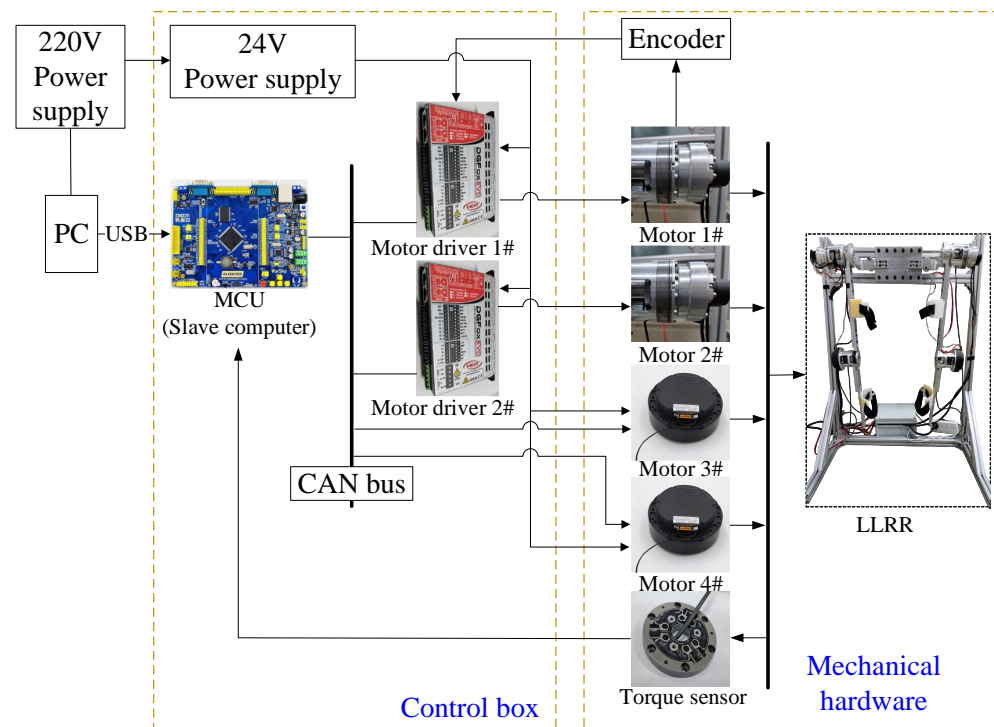


Figure 4. Flowchart of the control system.

Based on the developed control system, three different rehabilitation training modes have been developed, namely, passive exercise, active exercise and resistance exercise, respectively.

3.2. Passive Exercise

Passive exercise is suitable for the early stage of patient's rehabilitation training. At this stage, the LLRR needs to provide support and assist the patient's legs to walk according to the specified trajectory, thereby helping the patient to restore joints' ranges of motion and muscle strength. Generally speaking, passive exercise does not consider human's participation, and mainly relies on the robot to drive the patient's hip and knee joints to produce extension and flexion movement, which promotes the contraction and relaxation of lower limb muscles, tendons, ligaments, etc., and improves the activity of related tissues, prevents limb muscle atrophy.

The motion data of normal human's gait used in passive exercise comes from OpenSim software (developed by Stanford University), with one gait cycle 1 s. In order to obtain the tracking curve for training, the discrete data points in the gait are fitted by using MATLAB (MathWorks, Inc., Natick, Apple Hill Campus, MA, USA), and the coefficient that minimizes the residual error is found. The final equation of the design trajectory for passive exercise is as in (1). Considering that the gait speed of the patient during the rehabilitation process is low, the gait must be adjusted according to the actual rehabilitation needs. Therefore, the gait cycle of the LLRR is set to be 4 s, and the amplitude coefficient a , the frequency coefficient ω , the initial phase φ and the offset distance k in the standard gait are adjusted to obtain a suitable new gait.

$$\theta = \sum_{i=1}^n a_i \sin(\omega t + \varphi_i) + k \quad (1)$$

The fitting curves of the hip and knee joints can be obtained as shown in Figure 5. For the reason that the gait of the human body in the walking stage has periodicity and symmetry, the gait trajectory of the human body in the whole cycle can be deduced according to the acquired new gait.

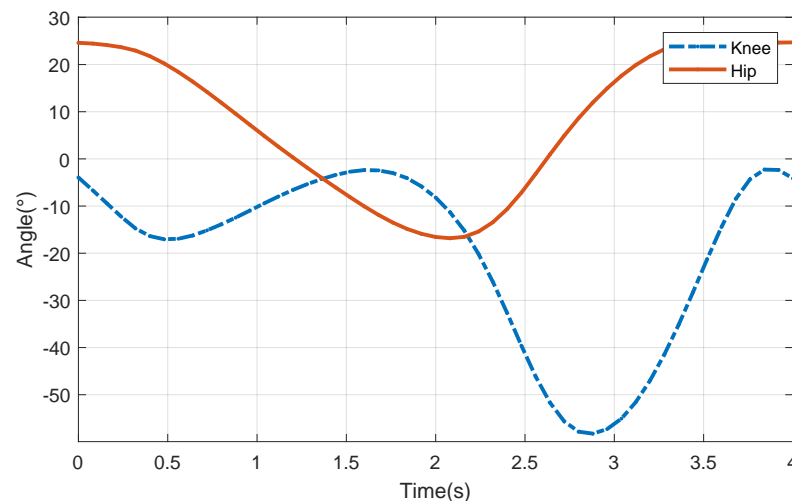


Figure 5. Fitting curve of hip and knee joints.

The multi-order trigonometric function expression of the hip joint is as in (2), while the function expression of the knee joint is as in (3).

$$\begin{aligned} \theta_{hip} = & 34.92 \sin(1.426t - 1.193) + 18.55 \sin(0.715t * 3.227) \\ & + 17.33 \sin(3.542t + 1.245) + 14.2 \sin(3.695t - 1.969) \\ & + 0.3362 \sin(8.412t - 4.345) + 0.178 \sin(11.58t - 2.154) \\ & + 0.1036 \sin(10.04t - 4.251) + 0.9214 \sin(5.891t + 1.713) \end{aligned} \quad (2)$$

$$\begin{aligned} \theta_{knee} = & 30.07 \sin(0.4836t - 1.153) + 17.19 \sin(3.113t - 1.093) \\ & + 3.568 \sin(4.922t - 0.4557) + 28.18 \sin(1.387t - 3.611) \\ & + 9.912 \sin(8.631t - 0.8891) + 9.351 \sin(8.831t - 1.928) \\ & + 0.886 \sin(6.843t - 0.8428) + 0.4085 \sin(16.87t + 1.202) \end{aligned} \quad (3)$$

The specific implementation method of passive exercise is as the following. First, we set the training mode as passive exercise mode in the human-robot interface (HRI) which is coded by using C#, convert the desired motion trajectory into the motion angle of each servo motor, and send the angle information to the MCU, and the MCU will convert the angle information to CANopen communication message and sent to the servo driver; then, the LLRR can be controlled to conduct passive exercise. At the same time, the joint motion information collected by the encoder is fed back to the control system to form a closed-loop control, so as to realize the real-time monitoring and tracking of the LLRR's motion trajectory. The flow chart of the passive exercise is shown as in Figure 6, where, θ , θ' and θ'' represent the motor joint angle, angular velocity and angular acceleration during the rehabilitation training process, respectively; e and T represent the angle error and human-robot interaction torque, respectively; the θ_r is the reference trajectory.

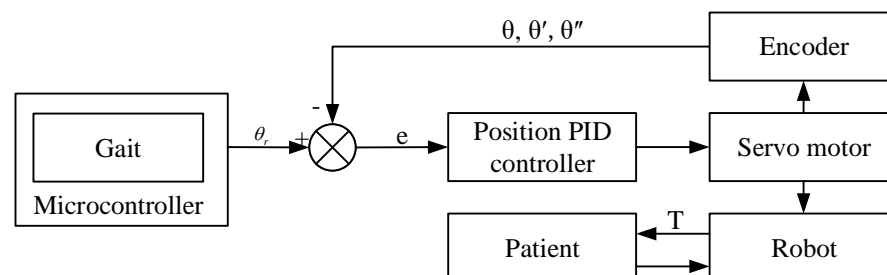


Figure 6. Flow chart of the passive exercise.

3.3. Active Exercise

The active exercise is suitable for the middle and later stages of the patient's rehabilitation training. At this time, the patient's intention of active participation is enhanced, and the patient has a certain ability of lower limb movement. The legs can walk, but the flexibility of the training needs to be ensured. During the active exercise, the human-robot torque is used as the excitation signal, and the output displacement of the motor makes the LLRR follow the movement of the legs, during which, the human-robot interaction torque is small, allowing the patient to perform large-scale movements and avoiding secondary damage caused by excessive interaction torque.

The proposed active exercise strategy includes two main aspects; one is the upper-level decision-making control system, which provides speed gain and position limit for the control strategy, inputs torque information to the controller, and outputs the target speed; The other is torque signal processing by using moving average filter and a second average filter to eliminate jumping points, and then input the torque value after filtering to the upper-level decision-making control system. The flow chart of the active exercise is shown as in Figure 7, where, the T_{in} is the interaction torque after filtering. During the active exercise, we set the training mode to the active exercise in the HRI; The interactive torque between the patient and the LLRR is measured and transmitted to the MCU for filtering operation, which is sent to the upper controller for analysis and processing combining with the gait information; the control system converts the input torque to the desired speed of joint motion, guiding the robot to follow the gait trajectory to follow the patient to complete the gait movement, which means that when the measured interaction torque is zero, the angular velocity becomes zero too, and the LLRR will stay where it is. By setting different coefficient between the interaction torque and the speed, different actual gait trajectories can be obtained under the same torque, so as to match different rehabilitation situations.

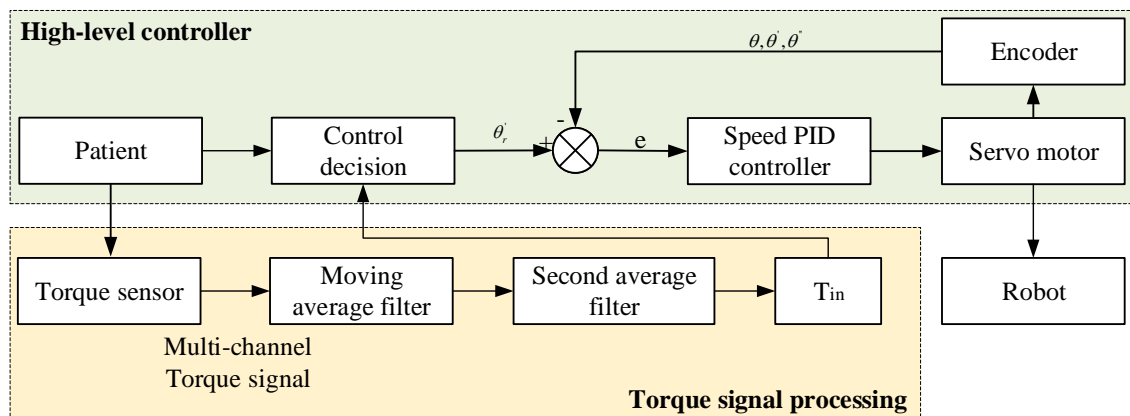


Figure 7. Flow chart of the active exercise.

3.4. Resistance Exercise

The resistance exercise is suitable for last stages of the patient's rehabilitation, which can be used to enhance the muscle strength; By resisting the resistance added from the robot, the motivation of rehabilitation training can be further stimulated, and thus increase the lower limb's muscle strength. For the LLRR, the position-based resistance control strategy is adopted, and the position control loop is corrected using the force signal as feedback. The specific implementation of the resistance exercise is as the follows. The human-robot interaction torque after processing is put into the resistance controller, which is the mapping between the interaction torque and the rotation angle; The resistance controller generates a deflection displacement relative to the initial position, and the deflection displacement depends on the size of the patient's active torque and the resistance parameter setting, which means that when the interaction torque is zero, the LLRR will return to its initial position. The resistance training control flow chart is shown in Figure 8.

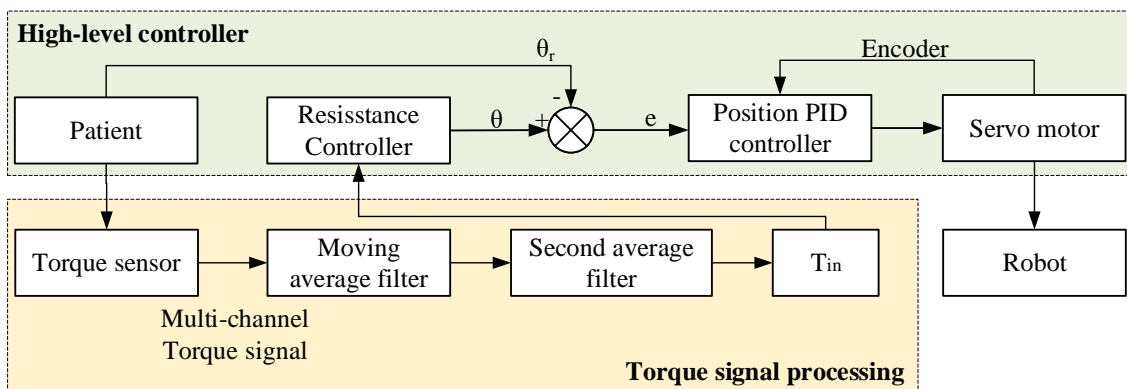


Figure 8. Flow chart of the resistance exercise.

4. Experiments and Results

To verify the effectiveness of the development of the different training modes of the developed LLRR, experiments were conducted with one voluntary healthy subject (male, 25 years old). The subject signed informed consent before the experiments. All experiments were approved by the Ethical Committee of Beijing University of Technology and conformed to the Declaration of Helsinki. During the experiments, the subject wore the LLRR on the treadmill, as shown in Figure 9, and the three different rehabilitation training modes have been tested in turn, respectively.

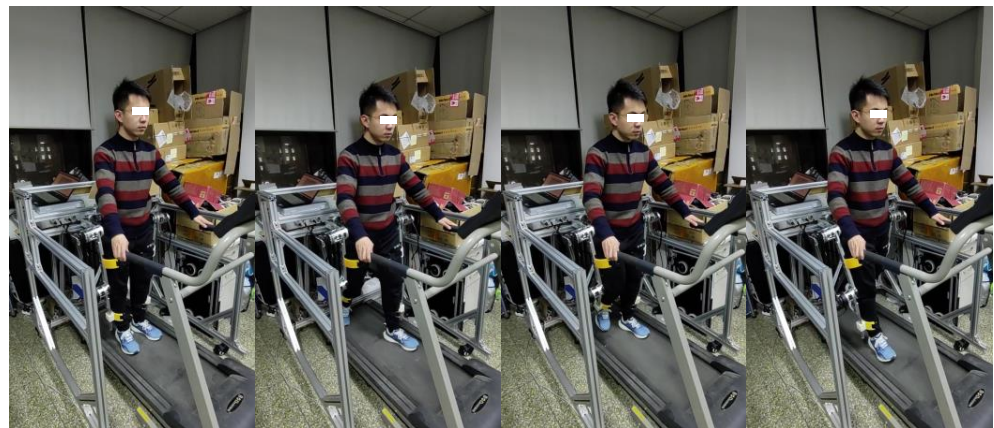


Figure 9. Subject on experiment with the LLRR.

4.1. Passive Exercise

During the passive exercise, the involved subject wore the developed LLRR at first, and LLRR drove the subject according to the fitting curve of hip and knee joints as in Figure 5, and the experimental results of the left hip joint and left knee joint are as in Figure 10, while the experimental results of the right hip joint and right knee joint are as in Figure 11, where, $LHip_{Tag}$, $RHip_{Tag}$, $LKnee_{Tag}$ and $RKnee_{Tag}$ represent the expected trajectories corresponding to the left hip joint, right hip joint, left knee joint, and right knee joint, respectively, and are derived from the normal gait curve of the human body based on the passive exercise strategy; $LHip_a$, $RHip_a$, $LKnee_{aRig}$ and $RKnee_{aRig}$ represent the real-time feedback angles from the encoders of the left hip joint, right hip joint, left knee joint and right knee joint respectively, all of which are rigidly driven trajectories without flexible units; $LKnee_a$ and $RKnee_a$ represent the real-time feedback trajectory tracking results of the encoders at the left and right knee joints with flexible elements, respectively; $FLHip$, $FRHip$, $FLKneeRig$ and $FRKneeRig$ are the real-time feedback torque values from the torque sensors at the left hip joint, right hip joint, left knee joint, and right knee joint, respectively, from one subject without flexible units; $FLKnee$ and $FRKnee$ are the real-time feedback torque values from the torque sensors at the left and right knee joints with flexible units, respectively.

From the results we can see that the LLRR can drive the subject along the preset trajectory no matter whatever the interaction torque is in the passive exercise mode. Also, under passive exercise, the expected trajectories of the hip joint $LHip_{Tag}$ and $RHip_{Tag}$ are similar to the actual trajectories $LHip_a$ and $RHip_a$, but in the movement of the knee joint, the movement with the flexible unit is more in line with the expected trajectory, and the control experiment without the flexible element can be seen from the torque values; The combined action of a rigid-flexible characteristics improves stability and better handles disturbances, reducing joint interaction torques.

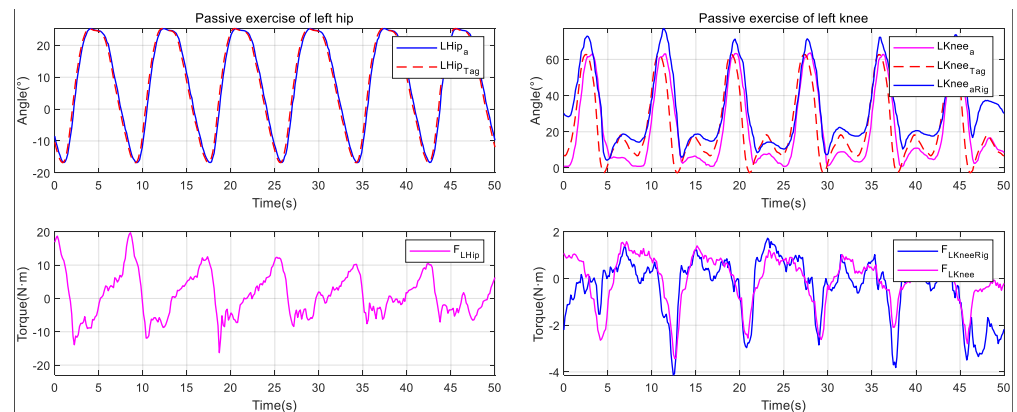


Figure 10. Passive exercise of left hip joint and knee joint.

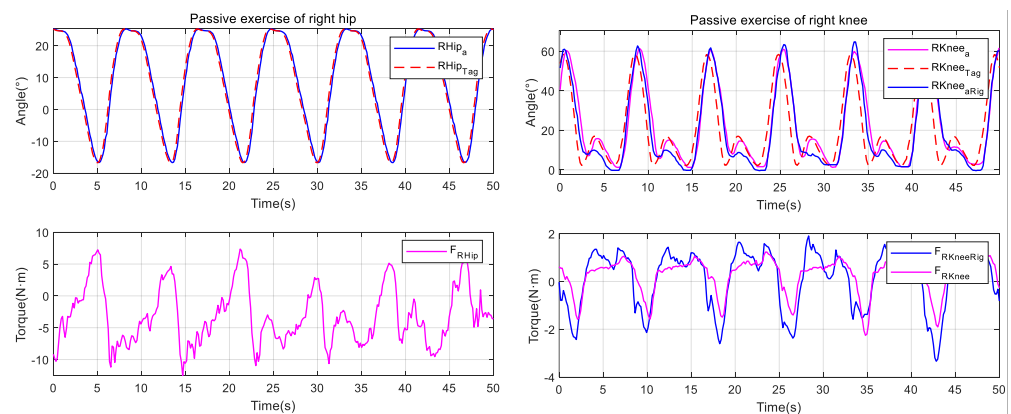


Figure 11. Passive exercise of right hip joint and knee joint.

4.2. Active Exercise

During the active exercise, the subject wore the developed LLRR, and the lower limb of the subject drove the robot to move as the subject intended. The threshold of the hip joint is set to be ± 2.5 N·m, while the threshold of the knee joint is set to be ± 0.7 N·m, according to the properties of different joints and test. The experimental results of the left hip joint and left knee joint shown as in Figure 12, while the experimental results of the right hip joint and right knee joint are as in Figure 13. From the results we can see that the trajectories of the hip joints and knee joints move in the direction of the interaction torques only if the detected torque exceeds the preset threshold, and we can see that the LLRR stays where it is at the previous moment if the detected torque at the current moment becomes zero (the detected torque is less than the preset threshold), showing good compliance and verifying the effectiveness of the developed rehabilitation training method.

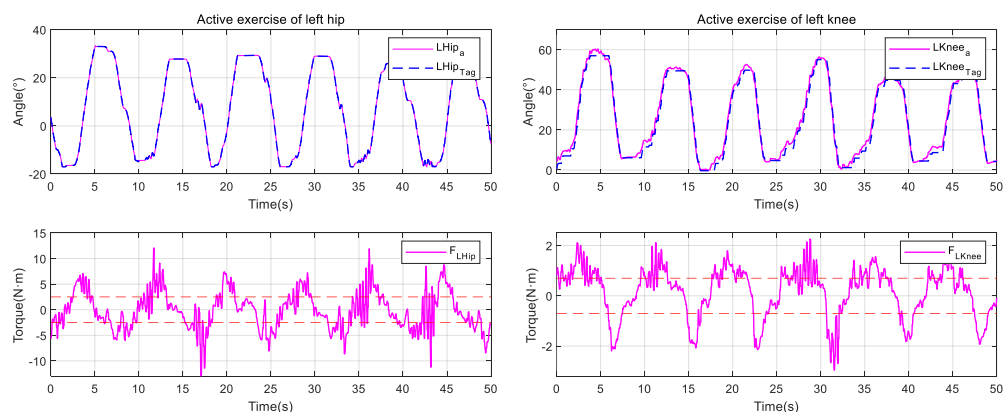


Figure 12. Active exercise of left hip joint and knee joint.

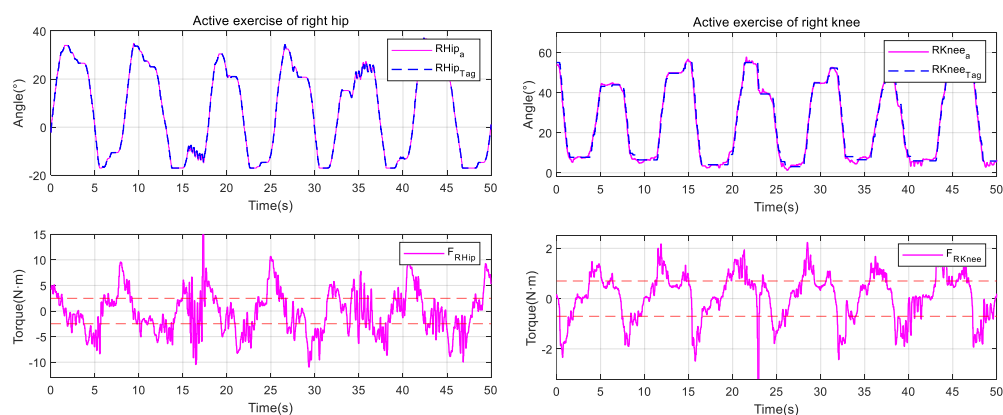


Figure 13. Active exercise of right hip joint and knee joint.

4.3. Resistance Exercise

During the resistance exercise, the subject actively exerts torques on the LLRR to resist its mechanical impedance, and if the interaction torque becomes zero, the LLRR will return to its initial position, just like a pendulum. The results of the resistance exercise of the left hip joint and left knee joint are shown as in Figure 14, while the experimental results of the right hip joint and right knee joint are as in Figure 15. From the results we can see that the when the detected torque is continuously exerted in the same direction, the deviation angle grows larger until reaching the limit position, and when the exerted torque remains unchanged at one position, the deviation angle similarly remains unchanged; When the exerted torque becomes zero, the LLRR returns to the initial equilibrium position. Also, under this exercise mode, the expected trajectory of the knee joint has the same trend as the actual trajectory under two trials with and without flexible units, but the difference between the two settings can be observed in the torque value; although suffering a loss of accuracy on part of the trajectory, the mechanically rigid-flexible mixing effect makes the human-machine interaction torque smaller. The results of the experiment verifies the effectiveness of the developed resistance exercise.

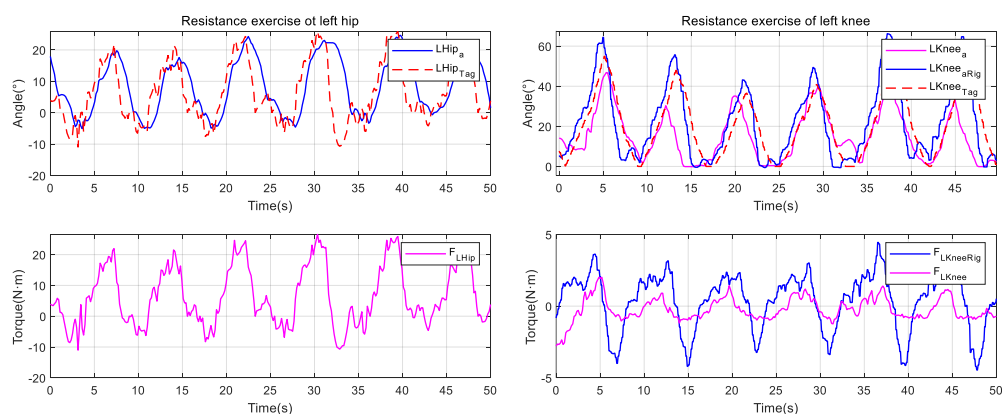


Figure 14. Resistance exercise of left hip joint and knee joint.

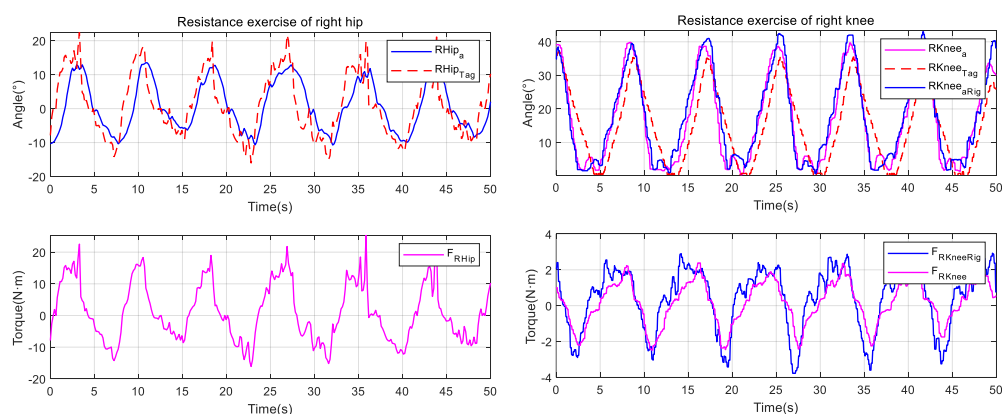


Figure 15. Resistance exercise of right hip joint and knee joint.

5. Conclusions

To improve the safety and comfort of robot-assisted lower limb rehabilitation, an LLRR with rigid-flexible characteristics and three different rehabilitation training methods was developed in this paper. The main contributions of the paper include: (1) Some passive joints is used to improve human-machine compatibility; (2) The design of flexible unit makes the mechanism have certain rigid-flexible characteristics; (3) Three different rehabilitation training methods have been developed to adapt to the patients in different stages of rehabilitation, which have been verified by recruiting healthy subjects with results showing good compatibility of the mechanism and good trajectory tracking performance of the developed training methods. In the future, more intelligent rehabilitation training methods combining with our previous studies on IMU inertial sensors [20,21] and the surface electromyography [22] will be developed to adapt to different patients and different recovery stages of the same patient, and the gravity compensation algorithm will be developed and added to improve the performance of the designed rehabilitation training methods; Also, a large number of experiments will be conducted with healthy subjects to ensure that the performance and stability of the developed LLRR are good enough for patients with lower limb dysfunction; and then the clinical trials on patients with lower limb disability will be conducted using our developed LLRR so that the device can be used in hospitals as soon as possible.

Author Contributions: Conceptualization, M.D. and J.L.; methodology, J.L.; software, J.Y.; validation, J.L.; formal analysis, M.D.; investigation, J.Y.; resources, M.D.; data curation, J.Y.; writing—original draft preparation, J.Y.; writing—review and editing, J.Y.; visualization, J.Y.; supervision, M.D.; project administration, M.D.; funding acquisition, M.D. All authors have read and agreed to the published version of the manuscript.

Funding: This work was supported in part by the National Key R&D Program of China under Grant No.2020YFC2004200, in part by the National Natural Science Foundation of China under Grants Nos.61903011 and 52175001, and in part by the General Program of Science and Technology Development Project of Beijing Municipal Education Commission under Grant No.KM202010005021.

Informed Consent Statement: Not applicable.

Institutional Review Board Statement: Not applicable.

Data Availability Statement: Not applicable.

Conflicts of Interest: The authors declare no conflict of interest.

References

1. Dong, M.J.; Zhou, Y.; Li, J.F.; Rong, X.; Fan, W.P.; Zhou, X.D.; Kong, Y. State of the art in parallel ankle rehabilitation robot: A systematic review. *J. Neuroeng. Rehabil.* **2021**, *18*, 52. [\[CrossRef\]](#)
2. Ochi, M.; Wada, F.; Saeki, S.; Hachisuka, K. Gait training in subacute non-ambulatory stroke patients using a full weight-bearing gait-assistance robot: A prospective, randomized, open, blinded-endpoint trial. *J. Neurol. Sci.* **2015**, *353*, 130–136. [\[CrossRef\]](#)
3. Meuleman, J.; Asseldonk, E.; Oort, G.; Rietman, H.; Kooij, H. LOPES II-Design and evaluation of an admittance controlled gait training robot with shadow-leg approach. *IEEE Trans. Neural Syst. Rehabil. Eng.* **2016**, *24*, 352–363. [\[CrossRef\]](#)
4. Banala, S.K.; Kim, S.H.; Agrawal, S.K.; Scholz, J.P. Robot assisted gait training with active leg exoskeleton (ALEX). *IEEE Trans. Neural Syst. Rehabil. Eng.* **2009**, *17*, 2–8. [\[CrossRef\]](#)
5. Esquenazi, A.; Talaty, M.; Packel, A.; Saulino, M. The ReWalk powered exoskeleton to restore ambulatory function to individuals with thoracic-level motor-complete spinal cord injury. *Am. J. Phys. Med. Rehabil.* **2012**, *91*, 911–921. [\[CrossRef\]](#)
6. Hartigan, C.; Kandilakis, C.; Dalley, S.; Clausen, M.; Wilson, E.; Morrison, S.; Etheridge, S.; Farris, R. Mobility outcomes following five training sessions with a powered exoskeleton. *Top. Spinal Cord Inj. Rehabil.* **2015**, *21*, 93–99. [\[CrossRef\]](#)
7. Zhou, L.B.; Chen, W.H.; Chen W.J.; Bai, S.P.; Zhang, J.B.; Wang, J.H. Design of a passive lower limb exoskeleton for walking assistance with gravity compensation. *Mech. Mach. Theory.* **2020**, *150*, 103840. [\[CrossRef\]](#)
8. Liu, D.X.; Xu, J.; Chen, C.J.; Long, X.G.; Tao, D.C.; Wu, X.Y. Vision-Assisted autonomous lower-limb exoskeleton robot. *IEEE Trans. Syst. Man Cybern. Syst.* **2021**, *51*, 3759–3770. [\[CrossRef\]](#)
9. Wang, L.P.; Tian, J.J.; Du, J.Z.; Zheng, S.Y.; Niu, J.Y.; Zhang, Z.Y.; Wu, J. A hybrid mechanism-based robot for end-traction lower limb rehabilitation: Design, analysis and experimental evaluation. *Machines* **2022**, *10*, 99. [\[CrossRef\]](#)
10. Nicholson-Smith, C.; Mehrabi, V.; Atashzar, S.F.; Patel, R. A multi-functional lower- and upper-limb stroke rehabilitation robot. *IEEE Trans. Med. Rob. Bionics.* **2020**, *2*, 549–552. [\[CrossRef\]](#)
11. Dawson-Elli, A.R.; Adamczyk, P.G. Design and validation of a lower-limb haptic rehabilitation robot. *IEEE Trans. Neural Syst. Rehabil. Eng.* **2020**, *28*, 1584–1594. [\[CrossRef\]](#)
12. Ma, Y.; Wu, X.Y.; Yang, S.X.; Dang, C.; Liu, D.X.; Wang, C.; Chen, C.J. Online gait planning of lower-limb exoskeleton robot for paraplegic rehabilitation considering weight transfer process. *IEEE Trans. Autom. Sci. Eng.* **2021**, *18*, 414–425. [\[CrossRef\]](#)
13. Hwang, B.; Oh, B.M.; Jeon, D. An optimal method of training the specific lower limb muscle group using an exoskeletal robot. *IEEE Trans. Neural Syst. Rehabil. Eng.* **2018**, *26*, 830–838. [\[CrossRef\]](#)
14. Amiri, M.S.; Ramli, R.; Aliman, N. Adaptive swarm fuzzy logic controller of multi-joint lower limb assistive robot. *Machines* **2022**, *10*, 425. [\[CrossRef\]](#)
15. Liu, L.; Leonhardt, S.; Ngo, C.; Misgeld, B.J.E. Impedance-controlled variable stiffness actuator for lower Limb robot applications. *IEEE Trans. Autom. Sci. Eng.* **2020**, *17*, 991–1004. [\[CrossRef\]](#)
16. Zhou, J.; Li, Z.; Li, X.; Wang, X.Y.; Song, R. Human-robot cooperation control based on trajectory deformation algorithm for a lower limb rehabilitation robot. *IEEE/ASME Trans. Mechatron.* **2021**, *26*, 3128–3138. [\[CrossRef\]](#)
17. Zhang, S.S.; Guan, X.; Ye, J.; Chen, G.; Zhang, Z.M.; Leng, Y.Q. Gait deviation correction method for gait rehabilitation with a lower limb exoskeleton robot. *IEEE Trans. Med. Rob. Bionics.* **2022**, *4*, 754–763. [\[CrossRef\]](#)
18. Li, J.F.; Cao, Q.; Dong, M.J.; Zhang, C.Z. Compatibility evaluation of a 4-DOF ergonomic exoskeleton for upper limb rehabilitation. *Mech. Mach. Theory.* **2021**, *156*, 104146. [\[CrossRef\]](#)
19. Dong, M.J.; Fan, W.P.; Li, J.F.; Zhou, X.D.; Rong, X.; Kong, Y.; Zhou, Y. A new ankle robotic system enabling whole-stage compliance rehabilitation training. *IEEE/ASME Trans. Mechatron.* **2021**, *26*, 1490–1500. [\[CrossRef\]](#)
20. Dong, M.J.; Yao, G.; Li, J.F.; Zhang, L.Y. Calibration of low cost IMU's inertial sensors for improved attitude estimation. *J. Intell. Rob. Syst.* **2020**, *100*, 1015–1029. [\[CrossRef\]](#)
21. Dong, M.J.; Fang, B.; Li, J.F.; Sun, F.C.; Liu, H.P. Wearable sensing devices for upper limbs: A systematic review. *Proc. Inst. Mech. Eng., Part H J. Eng. Med.* **2021**, *235*, 117–130. [\[CrossRef\]](#) [\[PubMed\]](#)
22. Li, J.F.; Zhou, Y.; Dong, M.J.; Jiao, R.; Jiang, L.W. Estimation of muscle activation during ankle rehabilitation. In Proceedings of the 2021 IEEE International Conference on Real-Time Computing and Robotics (RCAR), Qinghai, China, 15–19 July 2021.